Turkish Journal of Computer and Mathematics Education *Vol.11 No.03 (2020), 1361-1371*

Research Article

Trajectory Tracking Control for a Spatial Parallel Manipulator Based on Differential-Algebraic Equations

Tran Xuan Minh[a], Nguyen Van Quyen [b,*]

[a] Thai Nguyen University of Technology, No. 666, 3/2 Street, Thai Nguyen, Viet Nam
[b]Hanoi University of Science and Technology, Vietnam
[*]Corresponding Author.

Article History: Received: 10 October 2020; Revised: 28 October 2020; Accepted: 5 November 2020; Published online: 10 December 2020

Abstract: The motion equations of parallel spatial manipulators are a system of complicated differential-algebraic equations. Sothe construction of enough accurate and relatively simple mechanical models is needed. This paper introduces two mechanical models which can be used by control for the 3-PRS parallel manipulator. Using the methods as PD control, PID control to control 3-PRS parallel manipulator based on two different mechanical models is the article's main content. The simulation results showed PD control method, PID showed good results when using enough accurate mechanical models.

Keywords: Parallel manipulator, DAE, PD control, PID Control.

1. INTRODUCTION

Parallel manipulators are multi-body systems with a loop structure. Their motions are described by differential-algebraic equations [1-7]. In the works [8-13], the authors applied multi-body dynamics methods to calculate the plane and Delta spatial parallel manipulator dynamics. The tracking control of chain robots has been studied extensively [14-22]. However, controlling parallel manipulators to follow the desired trajectory has been rarely studied. In this paper, the authors present two mechanical models of the 3-PRS spatial Delta parallel manipulator, as shown in Figure 1. In the first model, we replace the parallelogram connecting bar mass with two-point masses. In model 2, the parallelogram connecting bar is replaced by a solid bar. Then, modern control methods are used to study the trajectory control problem of the 3-PRS spatial Delta parallel manipulator based on differential-algebraic equations.

2. DYNAMIC MODEL OF 3-PRS PARALLEL MANIPULATORS

According to the Grübler standard [3], the degree of freedom of the considered manipulator is f = 3. From the design model of the manipulator in Figure 1., we build the kinetic model of the manipulator as shown in Figure 2, in which the fixed machine table has vertices A_1, A_2, A_3 forming an equilateral triangle inscribed with the circle of radius r. Three sliders B_1, B_2, B_3 are solid objects with mass m1 moving in the vertical direction called driving stages. The positions of these stages are determined by their coordinates, d_1, d_2, d_3, respectively. The mass of the moving machine table is a solid object with a translational movement in the space, and its vertices D_1, D_2, D_3 form an equilateral triangle inscribed with radius r. The position of the moving table is determined by the coordinate x_P, y_P, z_P of point P. The three parallelograms, B_1D_1, B_2D_2, and B_3D_3, has weight m_2, linked with the sliders at B_1, B_2, and B_3 and linked to the moving table at D_1, D_2, D_3, respectively. For the sake of simplicity in system dynamics analysis, parallelogram stages are modeled by bars B_1D_1, B_2D_2, and B_3D_3. These bars of length l are connected to the stitches driven by Cardan joints and connected to the machine table by ball joints. These bars of length l are connected to the sliding driven stage by Cardan joints and connected to the moving table by ball joints. B_iD_i stages are positioned by angles θ_i, γ_i, as shown in Figure 3.

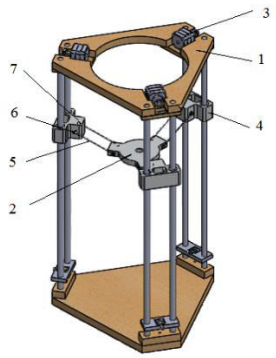

Figure 1. Design model of a Delta 3-PRS manipulator

(1. Fixed machine table, 2. Moving machine table, 3. Motor, 4. Sliding driven stage, 5. Connecting bar, 6-7. Ball joints or Cardan joints)

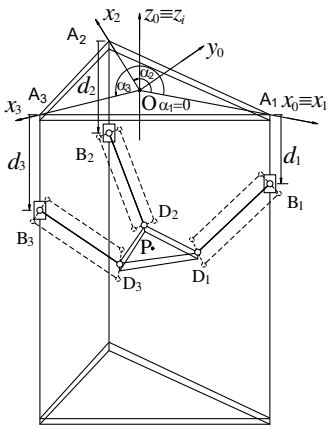

Figure 2. Robot kinematic diagram

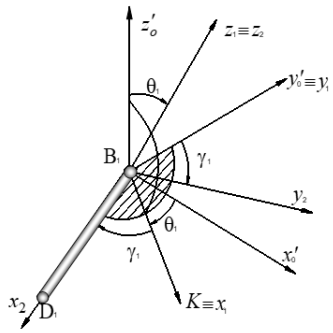

Figure 3. Positioning diagram of B_iD_i in the space

For the sake of simplicity in system dynamics analysis, parallelogram stages are modeled by bars B_1D_1, B_2D_2, and B_3D_3. These bars of length l are connected to the stitches driven by Cardan joints and connected to the machine table by ball joints. These bars of length l are connected to the sliding driven stage by Cardan joints and connected to the moving table by ball joints. B_iD_i stages are positioned by angles θ_i, γ_i, as shown in Figure 3. For convenience, the following symbols are included :

$$\mathbf{q}_a = \begin{bmatrix} d_1 & d_2 & d_3 \end{bmatrix}^T, \mathbf{q}_p = \begin{bmatrix} \theta_1 & \theta_2 & \theta_3 & \gamma_1 & \gamma_2 & \gamma_3 \end{bmatrix}^T, \mathbf{x} = \begin{bmatrix} x_P & y_P & z_P \end{bmatrix}^T \quad (1)$$

where $\mathbf{q}_a, \mathbf{q}_p, \mathbf{x}$ are the independent generalized coordinates of active joints, passive joints, and coordinates of the center P of the moving table B (manipulation coordinates). Thus, the generalized coordinates are $\mathbf{s} = \begin{bmatrix} \mathbf{q}_a^T & \mathbf{q}_p^T & \mathbf{x}^T \end{bmatrix}^T$.

3.KINEMATIC MODEL OF THE 3-PRS PARALLEL MANIPULATOR.

The kinematic model for the Delta 3-PRS parallel manipulator has been presented in this section will review the main results and analyze the difference between the two models.

Model 1: In this model, the parallelogram joints are replaced by solid bars whose mass is evenly distributed over the bar length. The weight and length of the bar are equal to the weight and length of the parallelogram joint.

Model 2: In this model, the parallelogram joints are replaced with weightless bars whose mass is concentrated at the bar's ends. The weight at each end of the bar is equal to half of the weight of the parallelogram.

Among the two models, Model 2 is straightforward, consisting of four solid translational objects, of which three drive sliders have an additional half of the parallelogram bar weight, and the moving table has an extra half of the mass of three parallelogram bars. So, to set up the motion equation of the manipulator, we choose the residual generalized coordinates as

$$\mathbf{s} = \begin{bmatrix} d_1 & d_2 & d_3 & x_P & y_P & z_P \end{bmatrix}^T \in \mathbb{R}^6 \tag{2}$$

Applying the Lagrange factor equation, we can establish the motion equation of the robot in the form of a matrix as below [3]:

$$\mathbf{M}(\mathbf{s})\ddot{\mathbf{s}} + \mathbf{C}(\mathbf{s}, \dot{\mathbf{s}})\dot{\mathbf{s}} + \mathbf{g}(\mathbf{s}) + \mathbf{\Phi}_s^T(\mathbf{s})\boldsymbol{\lambda} = \boldsymbol{\tau} \tag{3}$$

$$\mathbf{f}(\mathbf{s}) = \mathbf{0} \tag{4}$$

where:

$$\boldsymbol{\tau} = \begin{bmatrix} F_1 & F_2 & F_3 & 0 & 0 & 0 \end{bmatrix}^T;\ \boldsymbol{\lambda} = \begin{bmatrix} \lambda_1 & \lambda_2 & \lambda_3 \end{bmatrix}^T;\ \mathbf{\Phi}_s(\mathbf{s}) = \frac{\partial \mathbf{f}}{\partial \mathbf{s}} \in \mathbb{R}^{3\times 6}$$

$$\mathbf{M}(\mathbf{s}) = diag\begin{pmatrix} m_1 + \frac{1}{2}m_2,\ m_1 + \frac{1}{2}m_2,\ m_1 + \frac{1}{2}m_2, \\ m_P + \frac{3}{2}m_2,\ m_P + \frac{3}{2}m_2,\ m_P + \frac{3}{2}m_2 \end{pmatrix}$$

$$\mathbf{g}(\mathbf{s}) = -\begin{bmatrix} \left(m_1 + \frac{1}{2}m_2\right)g & \left(m_1 + \frac{1}{2}m_2\right)g & \left(m_1 + \frac{1}{2}m_2\right)g & 0 & 0 & \left(m_P + \frac{3}{2}m_2\right)g \end{bmatrix}^T$$

The constraint equations are established based on the following conditions:

$$(x_{Bi} - x_{Ei})^2 + (y_{Bi} - y_{Ei})^2 + (z_{Bi} - z_{Ei})^2 - l^2 = 0$$

Therefore, the constraint equations have the following form:

$f_i = l^2 - \left(\cos\alpha_i\left(R-r\right)-x_P\right)^2 - \left(\sin\alpha_i\left(R-r\right)-y_P\right)^2 - \left(d_i+z_P\right)^2 = 0$ with i=1, 2, 3

The matrix $\mathbf{C(s,\dot{s})}$ is calculated from the mass matrix $\mathbf{M(s)}$ using the Kronecker product as follows [6]:

$$\mathbf{C(s,\dot{s})} = \frac{\partial \mathbf{M(s)}}{\partial \mathbf{s}}(\mathbf{E}\otimes\dot{\mathbf{s}}) - \frac{1}{2}\left(\frac{\partial \mathbf{M(s)}}{\partial \mathbf{s}}(\dot{\mathbf{s}}\otimes\mathbf{E})\right)^T \tag{5}$$

where E is a unit matrix of the size of the vector s. Since $\mathbf{M}\left(\mathbf{s}\right)$ is a diagonal matrix whose elements are constants, $\mathbf{C(s,\dot{s})} = \mathbf{0}$.

If Model 1 is used, we have a mechanical system consisting of three sliders that drive the linear motion in the vertical direction, a moving table with a translational movement in space, and 3 bars, BiDi, solid objects moving in space. To position the bars we use the angles θ_i, γ_i as shown in Figure 3. Thus, to derive the motion equation, the residual generalized coordinates of the manipulator are selected as below:

$$\mathbf{s} = \left[d_1\ \theta_1\ \gamma_1\ d_2\ \theta_2\ \gamma_2\ d_3\ \theta_3\ \gamma_3\ x_P\ y_P\ z_P\right]^T \in \mathbb{R}^{12} \tag{6}$$

Applying the Lagrange factor equation, we can establish the motion equation of the manipulator in the matrix form as below [1]:

$$\mathbf{M(s)\ddot{s}} + \mathbf{C(s,\dot{s})\dot{s}} + \mathbf{g(s)} + \mathbf{\Phi}_s^T\mathbf{(s)\lambda} = \boldsymbol{\tau} \tag{7}$$

$$\mathbf{f(s)} = \mathbf{0} \tag{8}$$

Matrix $\mathbf{M(s)}$ is a square matrix of size 12×12 with the following form:

$$\mathbf{M(s)} = \begin{bmatrix} \mathbf{M}_1\mathbf{(s)} & \mathbf{0} & \mathbf{0} & \mathbf{0} \\ \mathbf{0} & \mathbf{M}_2\mathbf{(s)} & \mathbf{0} & \mathbf{0} \\ \mathbf{0} & \mathbf{0} & \mathbf{M}_3\mathbf{(s)} & \mathbf{0} \\ \mathbf{0} & \mathbf{0} & \mathbf{0} & \mathbf{M}_P\mathbf{(s)} \end{bmatrix} \tag{9}$$

where

$$\mathbf{M}_i\mathbf{(s)} = \begin{bmatrix} m_1+m_2 & \frac{1}{2}m_2 l\cos\theta_i\cos\gamma_i & -\frac{1}{2}m_2 l\sin\theta_i\sin\gamma_i \\ \frac{1}{2}m_2 l\cos\theta_i\cos\gamma_i & I_{cx}+\left(I_{cy}-I_{cx}+\frac{1}{4}m_2 l^2\right)\cos^2\gamma_i & 0 \\ -\frac{1}{2}m_2 l\sin\theta_i\sin\gamma_i & 0 & \frac{1}{4}m_2 l^2 + I_{cz} \end{bmatrix}$$

$\mathbf{M}_P\left(\mathbf{s}\right) = diag\left(m_P, m_P, m_P\right)$

The matrix $\mathbf{C(s,\dot{s})} \in \mathbb{R}^{12\times12}$ is calculated as follows:

$$\mathbf{C(s,\dot{s})} = \frac{\partial \mathbf{M(s)}}{\partial \mathbf{s}}(\mathbf{E}\otimes\dot{\mathbf{s}}) - \frac{1}{2}\left(\frac{\partial \mathbf{M(s)}}{\partial \mathbf{s}}(\dot{\mathbf{s}}\otimes\mathbf{E})\right)^T \tag{10}$$

Since $\mathbf{M}(\mathbf{s})$ contains non-constant elements, $\mathbf{C}(\mathbf{s},\dot{\mathbf{s}}) \neq \mathbf{0}$. The matrix g(s) has the following form:

$$\mathbf{g}(\mathbf{s}) = \left[\mathbf{g}_1(\mathbf{s})\ \mathbf{g}_2(\mathbf{s})\ \mathbf{g}_3(\mathbf{s})\ \mathbf{g}_P(\mathbf{s})\right]^T,$$

where

$$\mathbf{g}_i(\mathbf{s}) = \left[-(m_1+m_2)g \quad -\frac{1}{2}m_2 gl\cos\theta_i\cos\gamma_i \quad \frac{1}{2}m_2 gl\sin\theta_i\sin\gamma_i\right]^T \quad \mathbf{g}_P(\mathbf{s}) = \left[0\ 0\ m_P g\right]^T$$

for i =1, 2, 3.

The constraint equations are established based on the vector equations:

$$\overrightarrow{OA_i} + \overrightarrow{A_iB_i} + \overrightarrow{B_iD_i} + \overrightarrow{D_iP} = \overrightarrow{OP} \tag{11}$$

Project these equations on the coordinate system $Ox_0y_0z_0$, we obtain the following constraint equations:

$$\begin{aligned} x_P &= (R-r)\cos\alpha_i + l\cos\alpha_i\cos\theta_i\cos\gamma_i - l\sin\alpha_i\sin\gamma_i \\ y_P &= (R-r)\sin\alpha_i + l\sin\alpha_i\cos\theta_i\cos\gamma_i + l\cos\alpha_i\sin\gamma_i \\ z_P &= -d_i - l\sin\theta_i\cos\gamma_i \end{aligned} \tag{12}$$

for i = 1, 2, 3. Thus, we have nine constraint equations; therefore, $\mathbf{f}(\mathbf{s}) \in \mathbb{R}^9$. As a result, the matrix $\boldsymbol{F}_s(\mathbf{s})$ is calculated as

$$\boldsymbol{F}_s(\mathbf{s}) = \frac{\partial \mathbf{f}}{\partial \mathbf{s}} \in \mathbb{R}^{9\times 12} \tag{13}$$

The Lagrange factor vectors, $\boldsymbol{l}$ and $\boldsymbol{t}$, are given by :

$$\begin{aligned} \lambda &= \left[\lambda_1\ \lambda_2\ \lambda_3\ \lambda_4\ \lambda_5\ \lambda_6\ \lambda_7\ \lambda_8\ \lambda_9\right]^T \in \mathbb{R}^9, \\ \boldsymbol{\tau} &= \left[F_1\ 0\ 0\ F_2\ 0\ 0\ F_3\ 0\ 0\ 0\ 0\ 0\right]^T \in \mathbb{R}^{12} \end{aligned} \tag{14}$$

The motion equations of using Model 1 and Model 2 are both algebraic differential equations. We have the following comparison table:

Table 1. Motion equations of the robot based on 2 dynamic models.

	Model 1	Model 2
Number of degrees of freedom	3	3
Number of residual extrapolation coordinates	3x3 + 3 = 12	3 + 3 = 6
Number of associated equations	9	3
Number of Lagrange factor	9	3
Number of equations	21	9
M and C matrices	$\mathbf{M} = \mathbf{M}(\mathbf{s})$ $\mathbf{C}(\mathbf{s},\dot{\mathbf{s}}) \neq \mathbf{0}$	$\mathbf{M}(\mathbf{s}) = \text{const}$ $\mathbf{C}(\mathbf{s},\dot{\mathbf{s}}) = \mathbf{0}$

From the comparison table above, we see that the kinetic equation of Model 1 is relatively complex. Meanwhile, the kinetic equation of Model 2 is more straightforward.

4.METHODS OF TRAJECTORY TRACKING CONTROL FOR 3-PRS PARALLEL ROBOT

The motion equations of the two dynamic models are rewritten in the following general form [1-4] :

$$\mathbf{M}(\mathbf{s})\ddot{\mathbf{s}} + \mathbf{C}(\mathbf{s},\dot{\mathbf{s}})\dot{\mathbf{s}} + \mathbf{g}(\mathbf{s}) + \boldsymbol{\Phi}_s^T(\mathbf{s})\boldsymbol{\lambda} = \boldsymbol{\tau} \tag{15}$$

$$\mathbf{f}(\mathbf{s}) = \mathbf{0} \tag{16}$$

Where $\mathbf{M}(\mathbf{s}), \mathbf{C}(\mathbf{s},\dot{\mathbf{s}})$ are square matrices of size $n \times n$, $\boldsymbol{\Phi}_s(\mathbf{s})$ is a rectangular matrix of size $r \times n$. $\boldsymbol{\tau}$, $\mathbf{s}$ are column vectors with n elements, $\mathbf{f}$ are a column vectors with r elements. The residual constraint coordinates $\mathbf{s}$ and the actuation torque are written as.

Denoting $\boldsymbol{F}_a(\mathbf{s}) = \dfrac{\partial \mathbf{f}}{\partial \mathbf{q}_a}$; $\boldsymbol{F}_z(\mathbf{s}) = \dfrac{\partial \mathbf{f}}{\partial \mathbf{z}}$, the Jacobi matrix $\boldsymbol{F}_s(\mathbf{s})$ is rewritten as below:

$$\boldsymbol{F}_s(\mathbf{s}) = \left[\boldsymbol{F}_a(\mathbf{s}) \;\; \boldsymbol{F}_z(\mathbf{s})\right] = \partial \mathbf{f} / \partial \mathbf{s}\,.$$

According to [7], we define :

$$\mathbf{R}(\mathbf{s}) = \begin{bmatrix} \mathbf{E} \\ \boldsymbol{F}_z^{-1}(\mathbf{s})\boldsymbol{F}_a(\mathbf{s}) \end{bmatrix} \tag{17}$$

where $\mathbf{E}$ is a unit matrix of size $f \times f$.

We have:

$$\mathbf{R}^T(\mathbf{s})\boldsymbol{F}_s^T(\mathbf{s}) = \mathbf{0} \tag{18}$$

$$\dot{\mathbf{s}} = \mathbf{R}(\mathbf{s})\dot{\mathbf{q}}_a \tag{19}$$

Multiply the two sides of equation (15) by the matrix $\mathbf{R}^T(\mathbf{s})$ while simultaneously substituting equation (19) and its time derivative into equation (15), noting that $\boldsymbol{\tau}_z = \mathbf{0}$, we get :

$$\bar{\mathbf{M}}(\mathbf{s})\ddot{\mathbf{q}}_a + \bar{\mathbf{C}}(\mathbf{s},\dot{\mathbf{s}})\dot{\mathbf{q}}_a + \bar{\mathbf{g}}(\mathbf{s}) = \boldsymbol{\tau}_a \tag{20}$$

where:

$$\begin{aligned} \bar{\mathbf{M}}(\mathbf{s}) &:= \mathbf{R}^T(\mathbf{s})\mathbf{M}(\mathbf{s})\mathbf{R}(\mathbf{s}) \\ \bar{\mathbf{C}}(\mathbf{s},\dot{\mathbf{s}}) &:= \mathbf{R}^T(\mathbf{s})\left[\mathbf{M}(\mathbf{s})\dot{\mathbf{R}}(\mathbf{s},\dot{\mathbf{s}}) + \mathbf{C}(\mathbf{s},\dot{\mathbf{s}})\mathbf{R}(\mathbf{s})\right] \\ \bar{\mathbf{g}}(\mathbf{s}) &:= \mathbf{R}^T(\mathbf{s})\mathbf{g}(\mathbf{s}) \end{aligned} \tag{21}$$

According to [11], matrices $\bar{\mathbf{M}}(\mathbf{s}), \bar{\mathbf{C}}(\mathbf{s},\dot{\mathbf{s}})$ have the following properties: matrix $\bar{\mathbf{M}}(\mathbf{s})$ is a positive definite symmetric matrix, matrix $\dot{\bar{\mathbf{M}}}(\mathbf{s}) - 2\bar{\mathbf{C}}(\mathbf{s},\dot{\mathbf{s}})$ is a skewed symmetric matrix. We will use equation (20) and the above properties to design controllers for the Delta parallel robot.

4.1. PD controller

From the constraint equation **f(s)= 0,** solving the inverse kinematics problem, we obtain the desired position, velocity, and acceleration of the active joints of the robot $\mathbf{q}_a^d(t)$, $\dot{\mathbf{q}}_a^d(t)$, $\ddot{\mathbf{q}}_a^d(t)$. Denoting $\mathbf{q}_a(t)$, $\dot{\mathbf{q}}_a(t)$, $\ddot{\mathbf{q}}_a(t)$ as the actual position, velocity, and acceleration of the active joints of the robot. Then, the positional error has the following form :

$$\mathbf{e}(t) = \mathbf{q}_a(t) - \mathbf{q}_a^d(t) \tag{22}$$

We choose the control rule **u**(t) as below :

$$\mathbf{e}(\mathrm{t}) = \mathbf{q}_a(t) - \mathbf{q}_a^d(t) \to \mathbf{0} \tag{23}$$

with

$$\mathbf{v} = \ddot{\mathbf{q}}_a^d - \mathbf{K}_D\dot{\mathbf{e}} - \mathbf{K}_P\mathbf{e} \tag{24}$$

where $\mathbf{K}_D$, $\mathbf{K}_P$ are positive definite diagonal matrices:

$$\dot{V}(t) = \boldsymbol{n}^T\bar{\mathbf{M}}\dot{\boldsymbol{n}} + \frac{1}{2}\boldsymbol{n}^T\dot{\bar{\mathbf{M}}}\boldsymbol{n} + \sum_{i=1}^{n_a}\mathbf{w}_i^T\mathbf{w}_i \ , \ k_{Pi} > 0 \ , \ k_{Di} > 0$$

Substituting (23) and (24) into (20) yields:

$$\begin{aligned}\bar{\mathbf{M}}\left(\ddot{\mathbf{q}}_a^d - \mathbf{K}_D\dot{\mathbf{e}} - \mathbf{K}_P\mathbf{e}\right) + \bar{\mathbf{C}}\dot{\mathbf{q}}_a + \bar{\mathbf{g}} \\ = \bar{\mathbf{M}}\ddot{\mathbf{q}}_a + \bar{\mathbf{C}}\dot{\mathbf{q}}_a + \bar{\mathbf{g}}\end{aligned} \tag{25}$$

From (25) we have:

$$\bar{\mathbf{M}}\left[\ddot{\mathbf{e}} + \mathbf{K}_D\dot{\mathbf{e}} + \mathbf{K}_P\mathbf{e}\right] = \mathbf{0} \tag{26}$$

Since $\bar{\mathbf{M}}$ is a positive deterministic matrix, from (26) we have:

$$\ddot{\mathbf{e}} + \mathbf{K}_D\dot{\mathbf{e}} + \mathbf{K}_P\mathbf{e} = \mathbf{0} \tag{27}$$

Since $\mathbf{K}_D$, $\mathbf{K}_P$ are two diagonal matrices, from (27) we receive:

$$\ddot{e}_i + k_{Di}\dot{e}_i + k_{Pi}e_i = 0 \quad (i = 1,2,\ldots,n_a) \tag{28}$$

Define:

$$k_{Pi} = \omega_i^2, \ k_{Di} = 2\delta_i \tag{29}$$

Then, solution of (28) has the following form:

$$e_i(t) = A_i e^{-\delta_i t}\sin(\omega_i t + \alpha_i) \to 0 \ khi\, t \to \infty \tag{30}$$

If $\mathbf{K}_D$, $\mathbf{K}_P$ are chosen as diagonal matrices with positive elements, the system of differential equations (28) will be exponentially stable. Accordingly, $\mathbf{q}_a(t) \to \mathbf{q}_a^d(t)$. The control technique is straightforward. However, it is necessary to know precisely the matrices and vectors $\mathbf{M}_a$, $\mathbf{C}_a$, $\mathbf{g}_a$, $\mathbf{d}_a$, that is, to know precisely the model parameters. In other words, accurate model parameters are required.

4.2. PID controller

We choose the control rule u (t) as below

$$\mathbf{u}(t) = \bar{\mathbf{M}}(\mathbf{s})\mathbf{v} + \bar{\mathbf{C}}(\mathbf{s},\dot{\mathbf{s}})\dot{\mathbf{q}}_a + \bar{\mathbf{g}}(\mathbf{s}) \tag{31}$$

With

$$\mathbf{v} = \ddot{\mathbf{q}}_a^d - \mathbf{K}_D\dot{\mathbf{e}} - \mathbf{K}_P\mathbf{e} - \mathbf{K}_I\int_0^t \mathbf{e}d\tau \tag{32}$$

where $\mathbf{K}_D$, $\mathbf{K}_P$, $\mathbf{K}_I$ are positive definite diagonal matrices:

$$\mathbf{K}_P = diag\left(k_{P1},k_{P2},\ldots,k_{Pna}\right), \mathbf{K}_D = diag\left(k_{D1},k_{D2},\ldots,k_{Dna}\right), \mathbf{K}_I = diag\left(k_{I1},k_{I2},\ldots,k_{Ina}\right).$$

Substituting (31) and (32) into (20), noting that $\bar{\mathbf{M}}$ is a positive matrix, we obtain:

$$\ddot{\mathbf{e}} + \mathbf{K}_D\dot{\mathbf{e}} + \mathbf{K}_P\mathbf{e} + \mathbf{K}_I\int_0^t \mathbf{e}d\tau = \mathbf{0} \tag{33}$$

Taking derivative both sides of (33) w.r.t. time yields:

$$\dddot{\mathbf{e}} + \mathbf{K}_D\ddot{\mathbf{e}} + \mathbf{K}_P\dot{\mathbf{e}} + \mathbf{K}_I\mathbf{e} = \mathbf{0} \tag{34}$$

Since $\mathbf{K}_D, \mathbf{K}_P, \mathbf{K}_I$ are diagonal matrices, from (34), we deduce third-order differential equations as below:

$$\dddot{e}_{ai} + k_{Di}\ddot{e}_{ai} + k_{Pi}\dot{e}_{ai} + k_{Ii}e_{ai} = 0 \quad (i=1,2,\ldots,n_a) \tag{35}$$

Equations (35) are the linear differential equations of the constant coefficient. Characteristic equations take the following form:

$$\lambda_i^3 + k_{Di}\lambda_i^2 + k_{Pi}\lambda_i + k_{Ii} = 0. \quad (i=1,2,\ldots,\ n_a) \tag{36}$$

According to the Hurwitz stability criteria, the conditions for characteristic equation solutions to have a negative part are:

$$k_{Di} > 0,\ k_{Pi} > 0,\ k_{Ii} > 0,\ k_{Di}k_{Pi} - k_{Ii} > 0 \ (i = 1,2,\ldots,\ n_a) \tag{37}$$

Thus, if the coefficients are chosen such that the conditions (37) are satisfied, the differential equations (35) will be exponentially stable. Therefore, $\mathbf{q}_a(t) \to \mathbf{q}_a^d(t)$.

5.NUMERICAL SIMULATION

This section performs the simulation of 3-PRS parallel manipulator control system on Matlab\Simulink.The parameters of the manipulator are given as below:

$$l = 0.242;\ R = 0.16;\ r = 0.029\ (m);$$
$$\alpha_1 = 0;\ \alpha_2 = 2\pi/3;\ \alpha_3 = 4\pi/3;$$
$$m_1 = 0.12;\ m_2 = 2\times 0.15;\ m_P = 0.2(kg);$$
$$\mathbf{I}_{1c} = diag(0,\ ml^2/12,\ ml^2/12)$$

The controller parameters are selected as below:

PD controller: $\mathbf{K}_P = 2500\,\text{diag}(1,1,1);$ $\mathbf{K}_D = 150\,\text{diag}(1,1,1);$

PID controller: $\mathbf{K}_P = 2500\,\mathrm{diag}(1,1,1); \mathbf{K}_I = 250\,\mathrm{diag}(1,1,1); \mathbf{K}_D = 150\,\mathrm{diag}(1,1,1);$

The trajectory of the moving table is given as below:

$x_P = -0.05\cos(2\pi t);\ y_P = 0.05\sin(2\pi t); z_P = -0.5(m)$

The model uncertainty is 20%, and there is noise as below:

$$\mathbf{d}(\mathbf{s}) = \frac{1}{3}[\sin 20t \quad \cos 20t \quad \sin 20t \quad \cos 20t ...]^T_{1\times 12}$$

The control diagram for the manipulator is shown in Figure 4.

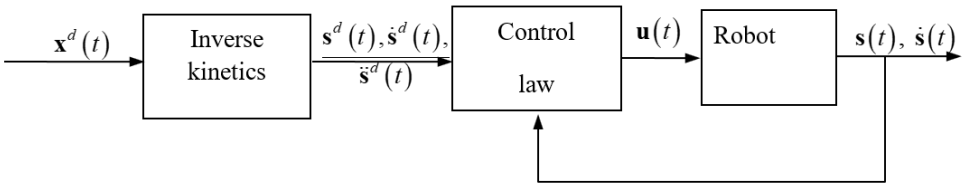

Figure 4. *Control diagram*

Simulation results for 3-PRS Delta parallel manipulator are shown in Figures 5. and Figures 6.

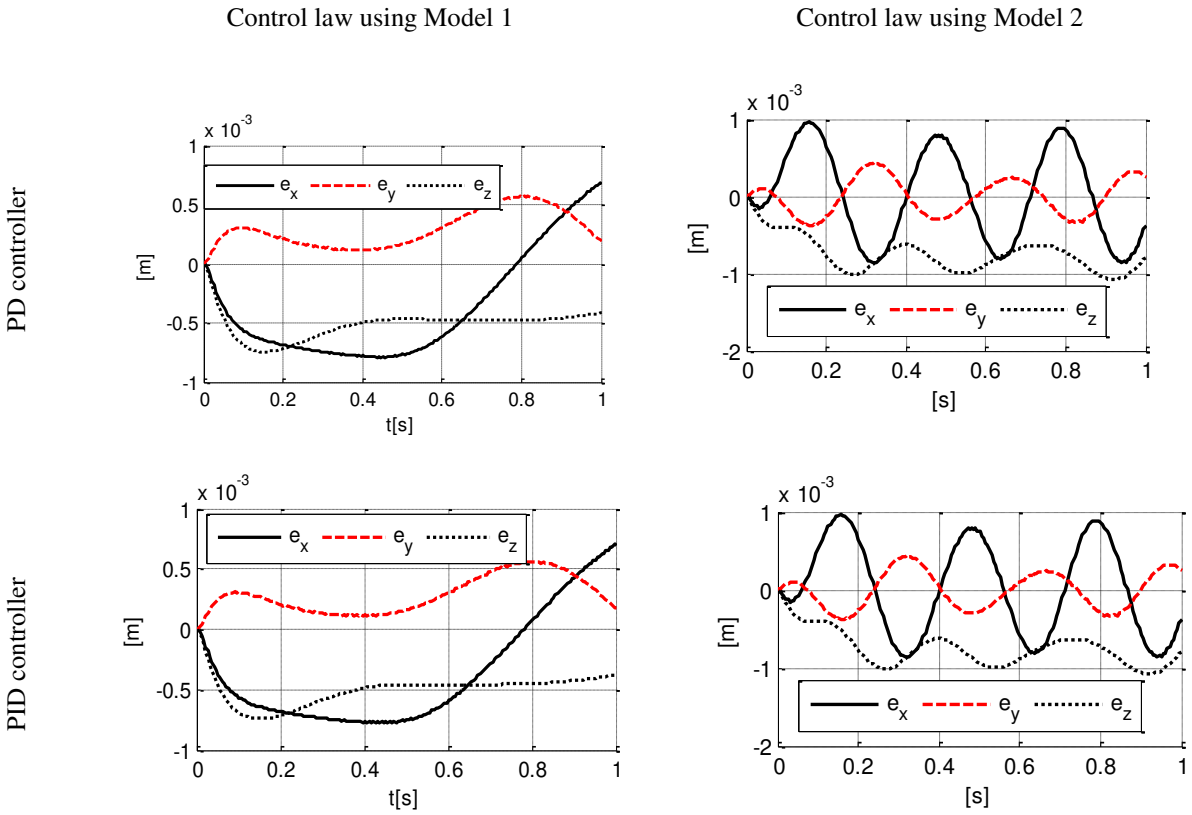

Figure 5. *Position error of the moving table usind different controllers*

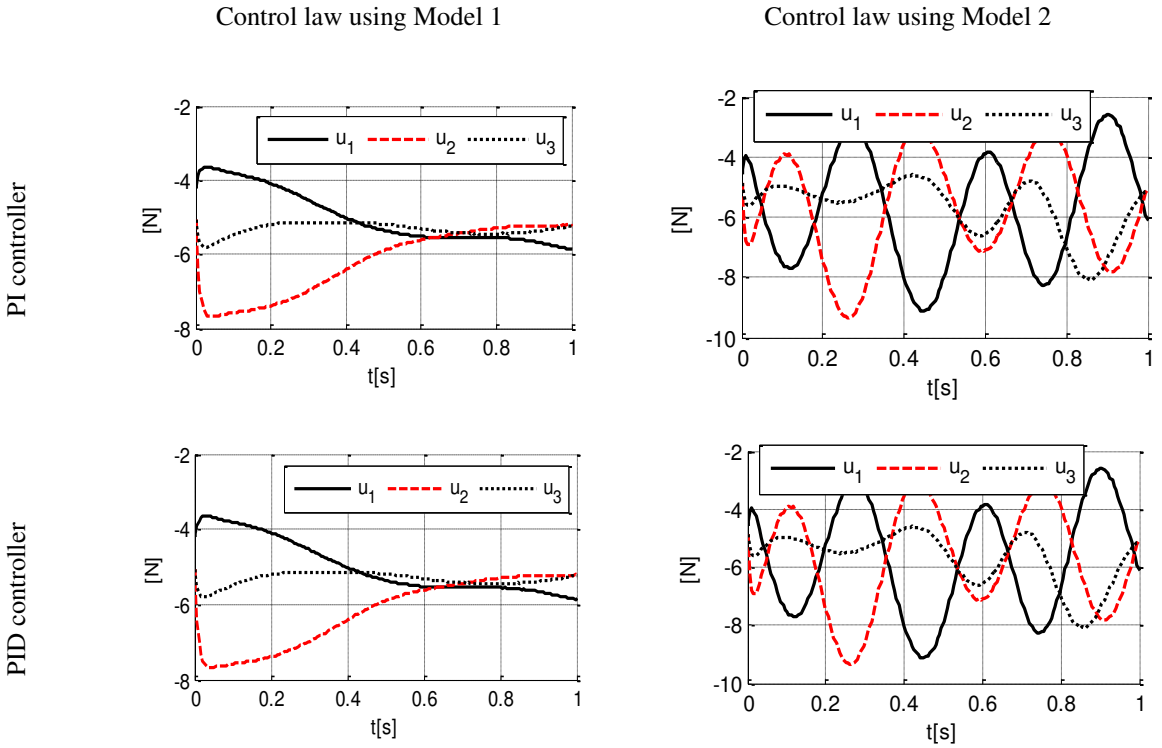

Figure 6. *Torque control*

The control rules based on Model 2 (the point mass model) are much more straightforward than those based on Model 1 (the solid-body model) because the kinetic equations of the point mass model are much simpler and more compact than the kinetic equations of the solid body model, as shown in Table 1.When using PD, PID control rules to control a real robot based on the model, both models give equally inaccurate efficiency, about 10-3 m, as depicted in Figure 5. Figure 6.

6.CONCLUSION

This paper presents the construction of controllers for parallel manipulators based on a system of algebraic differential equations. Below are some conclusions about modeling and controlling Delta 3-PRS space parallel manipulator. The differential-algebraic equations describing the Delta parallel manipulator's motion based on Model 2 are much simpler than those based on Model 1. When the PD and PID control laws are used, the obtained results based on Model 2 are worse than those based on Model 1.

ACKNOWLEDGEMENTS

The authors gratefully acknowledge the Thai Nguyen University of Technology for supporting this work.

REFERENCES

1.De Jalon, J. G., & Bayo, E. (2012). *Kinematic and dynamic simulation of multibody systems: the real-time challenge*. Springer Science & Business Media.

2. Tsai, L. W. (1999). Robot analysis: the mechanics of serial and parallel manipulators. John Wiley & Sons.

3. Merlet, J. P., Gosselin, C., & Huang, T. (2016). Parallel mechanisms. In *Springer handbook of robotics* (pp. 443-462). Springer, Cham.
4. Ceccarelli, M. (2004). Fundamentals of the mechanics of robots. In *Fundamentals of Mechanics of Robotic Manipulation* (pp. 73-240). Springer, Dordrecht.
5. Van Khang, N. (2010). Consistent definition of partial derivatives of matrix functions in dynamics of mechanical systems. *Mechanism and Machine Theory*, *45*(7), 981-988.
6. Van Khang, N. (2011). Kronecker product and a new matrix form of Lagrangian equations with multipliers for constrained multibody systems. *Mechanics Research Communications*, *38*(4), 294-299.
7. Blajer, W., Schiehlen, W., & Schirm, W. (1994). A projective criterion to the coordinate partitioning method for multibody dynamics. *Archive of Applied Mechanics*, *64*(2), 86-98.
8. Brinker, J., Corves, B., & Wahle, M. (2015, October). A comparative study of inverse dynamics based on clavel's delta robot. In *Proceedings of the 14th World Congress in Mechanism and Machine Science. Taipei, Taiwan* (pp. 25-30).
9. Geike, T., & McPhee, J. (2003). Inverse dynamic analysis of parallel manipulators with full mobility. *Mechanism and Machine Theory*, *38*(6), 549-562.
10. Staicu, S. (2009). Inverse dynamics of the 3-PRR planar parallel robot. *Robotics and Autonomous Systems*, *57*(5), 556-563.
11. Müller, A., & Hufnagel, T. (2012). Model-based control of redundantly actuated parallel manipulators in redundant coordinates. *Robotics and Autonomous systems*, *60*(4), 563-571.
12. Van Khang, N., & Tuan, L. A. (2013). On the sliding mode control of redundant parallel robots using neural networks. In *Proc. of the 3th IFToMM International Symposium on Robotics and Mechatronics, Singapore, Research Publishing* (pp. 168-177).
13. Asgari, M., Ardestani, M. A., & Asgari, M. (2013, February). Dynamics and control of a novel 3-DoF spatial parallel robot. In *2013 First RSI/ISM International Conference on Robotics and Mechatronics (ICRoM)* (pp. 183-188). IEEE.
14. Sciavicco, L., & Siciliano, B. (2000). Interaction control. In *Modelling and Control of Robot Manipulators* (pp. 271-294). Springer, London.
15. Kelly, R., Davila, V. S., & Perez, J. A. L. (2006). *Control of robot manipulators in joint space*. Springer Science & Business Media.
16. Slotine, J. J. E., & Li, W. (1991). *Applied nonlinear control* (Vol. 199, No. 1). Englewood Cliffs, NJ: Prentice hall.
17. Utkin, V. I. (1992). Sliding modes in optimization and control problems.
18. Cat, P. T., & Hiep, N. T. (2009, August). Robust PID sliding mode control of robot manipulators with online learning neural network. In *2009 European Control Conference (ECC)* (pp. 2187-2192). IEEE.
19. Sun, F., Sun, Z., & Woo, P. Y. (2001). Neural network-based adaptive controller design of robotic manipulators with an observer. *IEEE Transactions on Neural networks*, *12*(1), 54-67.
20. Barambones, O., & Etxebarria, V. (2002). Robust neural control for robotic manipulators. *Automatica*, *38*(2), 235-242.
21. Wai, R. J. (2003). Tracking control based on neural network strategy for robot anipulator. *Neurocomputing*, *51*, 425-445.
22. Jiang, Z. H. (2010). Trajectory control of robot manipulators using a neural network controller. *Robot Manipulators Trends and Development*, 361-376.